Available online at www.sciencedirect.com
SCIENCE DIRECT®
Journal of Sound and Vibration 292 (2006) 461–473
JOURNAL OF SOUND AND VIBRATION
www.elsevier.com/locate/jsvi

Smooth orthogonal decomposition-based vibration mode identification

David Chelidze*, Wenliang Zhou

Department of Mechanical Engineering and Applied Mechanics, 203 Wales Hall, 92 Upper College Road, University of Rhode Island, Kingston, RI 02881, USA

Received 8 November 2004; received in revised form 13 July 2005; accepted 3 August 2005
Available online 3 November 2005

Abstract

A new multivariate data analysis method called *smooth orthogonal decomposition* (SOD) is proposed to extract linear normal modes and natural frequencies of multi-degree-of-freedom and distributed-parameter vibration systems. It is demonstrated that for an undamped free vibration of a multi-degree-of-freedom system, the computed smooth orthogonal modes are in direct correspondence with the actual normal vibration modes and the smooth orthogonal values are related to the corresponding natural frequencies. The same is also shown to be true for lightly damped free vibrations of both lumped- and distributed-parameter systems. In contrast to the intrinsic limitations of the *proper orthogonal decomposition* (POD) analysis, which requires the knowledge of system's mass matrix to extract normal modes and cannot uniquely identify modal subspaces that have similar proper orthogonal values, the SOD is shown to overcome both of these deficiencies. Numerical examples are provided to compare the performances of the POD- and SOD-based modal identification in various types of vibration environment.

1. Introduction

This paper is about a new multivariate data analysis method called *smooth orthogonal decomposition* (SOD) and its application in extracting *linear normal modes* (LNMs) of multi-degree-of-freedom and distributed parameter vibration systems. The new method overcomes major deficiencies inherent in the POD when applied to structural vibration analysis. In contrast with the POD, the SOD does not require an a priori knowledge of system's mass matrix for modal identification. Furthermore, it also overcomes the POD's characteristic limitation that the principal directions or *proper orthogonal modes* (POMs) are not uniquely defined for comparable *proper orthogonal values* (POVs). In addition, the SOD-based identification also provides accurate estimates of natural frequencies for the identified LNMs.

The POD, also known as Karhunen–Loève decomposition, principal component analysis or singular-value decomposition is a powerful multivariate statistics method and has been widely used in engineering areas

*Corresponding author. Tel.: +1 401 874 2356; fax: +1 401 874 2355.
E-mail address: chelidze@egr.uri.edu (D. Chelidze).
URL: http://www.mce.uri.edu/chelidze/.

0022-460X/$ - see front matter © 2005 Elsevier Ltd. All rights reserved.
doi:10.1016/j.jsv.2005.08.006

to capture the dominant components or modes. In nonlinear dynamics field, the POD has been used to extract the dimension information from an embedded attractor [1,2]. In signal processing, the POD is employed to identify subspaces to which clean orbits are constrained [3–5]. In turbulent flow analysis, Holmes et al. [6] used the POD to extract energy coherent structures from turbulent velocity fields.

In structural vibration areas, recent efforts are directed towards relating POMs to LNMs of vibration systems. Feeny and his colleagues have been particularly active in this field. In Ref. [7], Feeny and Kappagantu report that for a discrete vibration system, the POMs of simulated vibration data converge to the LNMs in the undamped free vibration case. Kerschen and Golinval [8] reach a similar conclusion by employing the singular-value decomposition. In a later work, Feeny [9] extends the above results to a continuous vibration system. Feeny and Liang [10] extend the POD results to the random excitation environment to address multimode free vibration problems. These new findings provide a promising alternative to the traditional modal analysis since there is no need to measure the external force as it is required for frequency domain modal analysis. However, in practical applications of the POD there are several limitations that need to be overcome. The first problem is that the discrete normal vibration modes are orthogonal with respect to the mass matrix of the system, while the POMs are orthogonal with respect to each other. In Ref. [7], it is shown that if a raw vibration data is pre-multiplied by the corresponding mass matrix the resulting POMs will approximate actual vibration modes. Therefore for practical purposes, the mass matrix has to be known a priori. The second problem is related to an inherent shortcoming of the POD, that is, for two comparable POVs the corresponding POMs are not uniquely defined. In vibration analysis, this translates into the following problem: when the system's response contains two LNMs, whose coordinates have comparable oscillation amplitudes, the POD will not be able to differentiate them. In Ref. [11], Han and Feeny state that for a system in resonance one can use raw vibration data in the POD analysis to extract the vibration mode in resonance and proposed a filter-based POD technique to extract the other desired vibration modes.This makes it possible to successfully extract the desired mode if the raw time series contain only corresponding frequency information but the frequency domain analysis is still required.

In Section 2 the SOD and some of its properties are described. The applications of the SOD to a multi-degree-of-freedom free vibration system for undamped and lightly damped cases are presented in more detail. A multi-degree-of-freedom forced vibration and a distributed-parameter vibration cases are also investigated. The numerical results are given and compared with those given in Ref. [7]. We conclude with the discussion and summary of the results.

2. Smooth orthogonal decomposition

The basic idea of the SOD derives from the *optimal tracking* idea advocated in Ref. [12], where a scalar damage observer was proposed. It was further developed into the SOD for multidimensional damage identification and slow-time trajectory reconstruction in a hierarchical dynamical system [13,14]. The idea is that given noisy multivariate measurements that contain some deterministic (i.e., smooth in time) signals one needs to look for the projections that are smooth in time to identify deterministic trends. At the same time one needs to require the maximum possible variance of the projections to eliminate constant projections. In what follows, for completeness, we provide a brief derivation of the SOD and emphasize some of its properties that are in contrast with the POD.

2.1. The SOD derivation

Given a sampled scalar field in the form of a matrix $\mathbf{X} \in \mathbb{R}^{n\times m}$, where each column contains a scalar time series of measurement taken at m different spatial locations sampled using a constant Δt sampling period, we are looking for a linear projection of that matrix $\mathbf{q} = \mathbf{X}\boldsymbol{\phi}$, where $\boldsymbol{\phi} \in \mathbb{R}^{m\times 1}$ and $\mathbf{q} \in \mathbb{R}^{n\times 1}$, such that this projection keeps not only the maximum possible variance of the original field, but is also as smooth in time as possible.

To describe the smoothness of the projected field, we introduce a $(n-1)\times n$ differential operator

$$\mathbf{D}=\frac{1}{\Delta t}\begin{bmatrix}-1 & 1 & 0 & \dots & 0\\ 0 & -1 & 1 & \dots & 0\\ \vdots & \ddots & \ddots & \ddots & \vdots\\ 0 & \dots & 0 & -1 & 1\end{bmatrix}$$

and use the approximate velocity matrix $\mathbf{V}=\mathbf{DX}$ as the matrix that describes the time fluctuations in $\mathbf{X}$. Thus, the SOD idea translates into the following constrained maximum variance problem:

$$\max_{\boldsymbol{\phi}}\|\mathbf{X}\boldsymbol{\phi}\|^2 \text{ subject to } \min_{\boldsymbol{\phi}}\|\mathbf{V}\boldsymbol{\phi}\|^2 \quad \text{or} \quad \max_{\boldsymbol{\phi}}\left\{\lambda(\boldsymbol{\phi})=\frac{\|\mathbf{X}\phi\|^2}{\|\mathbf{V}\phi\|^2}\right\}, \tag{1}$$

where the mean has been subtracted from the columns of the matrices $\mathbf{X}$ and $\mathbf{V}$. Now the numerator of the above expression can be written as

$$\|\mathbf{X}\boldsymbol{\phi}\|^2=(\mathbf{X}\boldsymbol{\phi})^{\mathrm{T}}\mathbf{X}\boldsymbol{\phi}=\boldsymbol{\phi}^{\mathrm{T}}(\mathbf{X}^{\mathrm{T}}\mathbf{X})\boldsymbol{\phi}=n\,\boldsymbol{\phi}^{\mathrm{T}}\boldsymbol{\Sigma}_{\mathbf{X}}\boldsymbol{\phi}, \tag{2}$$

where $\boldsymbol{\Sigma}_{\mathbf{X}}$ is the covariance matrix of $\mathbf{X}$. Similarly, we can show that $\|\mathbf{V}\boldsymbol{\phi}\|^2=(n-1)\,\boldsymbol{\phi}^{\mathrm{T}}\boldsymbol{\Sigma}_{\mathbf{V}}\boldsymbol{\phi}$, where $\boldsymbol{\Sigma}_{\mathbf{V}}$ is the covariance matrix of $\mathbf{V}$. Both of these matrices are numerical approximations of the corresponding true covariance matrices. Thus, Eq. (1) becomes the following *Rayleigh's quotient* problem:

$$\max_{\boldsymbol{\phi}}\left\{\lambda(\boldsymbol{\phi})=\frac{\boldsymbol{\phi}^{\mathrm{T}}\boldsymbol{\Sigma}_{\mathbf{X}}\boldsymbol{\phi}}{\boldsymbol{\phi}^{\mathrm{T}}\boldsymbol{\Sigma}_{\mathbf{V}}\boldsymbol{\phi}}\right\}. \tag{3}$$

In order to obtain the stationary point of Eq. (3) we differentiate it with respect to $\boldsymbol{\phi}$, to obtain

$$\nabla\lambda(\boldsymbol{\phi})=0=\frac{2(\boldsymbol{\phi}^{\mathrm{T}}\boldsymbol{\Sigma}_{\mathbf{V}}\boldsymbol{\phi})\boldsymbol{\Sigma}_{\mathbf{X}}\boldsymbol{\phi}-2(\boldsymbol{\phi}^{\mathrm{T}}\boldsymbol{\Sigma}_{\mathbf{X}}\boldsymbol{\phi})\boldsymbol{\Sigma}_{\mathbf{V}}\boldsymbol{\phi}}{(\boldsymbol{\phi}^{\mathrm{T}}\boldsymbol{\Sigma}_{\mathbf{V}}\boldsymbol{\phi})^2}. \tag{4}$$

Thus, the SOD problem is transformed into a *generalized eigenvalue problem*

$$\boldsymbol{\Sigma}_{\mathbf{X}}\boldsymbol{\phi}_i=\lambda_i\boldsymbol{\Sigma}_{\mathbf{V}}\boldsymbol{\phi}_i, \quad i=1,\dots,m, \tag{5}$$

where λ_i are the generalized eigenvalues or *smooth orthogonal values* (SOVs) and $\boldsymbol{\phi}_i$ are generalized eigenvectors or *smooth orthogonal modes* (SOMs). By projecting our matrix $\mathbf{X}$ onto the SOMs we obtain *smooth orthogonal coordinates* (SOCs) $\mathbf{q}_i$, whose degree-of-smoothness is described by the magnitude of SOVs, refer to Eq. (1), higher values yielding smoother coordinates.

2.2. Basic properties of the SOD

One of the basic properties of the SOD, which is not shared by the POD, is that it is invariant with respect to an invertible linear coordinate transformation. In other words the SOD of $\mathbf{X}$ and $\mathbf{Y}=\mathbf{XR}$ yield the same SOCs, if the matrix $\mathbf{R}\in\mathbb{R}^{m\times m}$ is invertible. To illustrate this property, the SOD problem for $\mathbf{Y}=\mathbf{XR}$ is written as

$$(\mathbf{XR})^{\mathrm{T}}\mathbf{XR}\tilde{\boldsymbol{\phi}}_i=\tilde{\lambda}_i(\mathbf{DXR})^{\mathrm{T}}\mathbf{DXR}\tilde{\boldsymbol{\phi}}_i, \quad i=1,\dots,m, \tag{6}$$

which translates into

$$\mathbf{R}^{\mathrm{T}}\boldsymbol{\Sigma}_{\mathbf{X}}\mathbf{R}\tilde{\boldsymbol{\phi}}_i=\tilde{\lambda}_i\mathbf{R}^{\mathrm{T}}\boldsymbol{\Sigma}_{\mathbf{V}}\mathbf{R}\tilde{\boldsymbol{\phi}}_i, \quad i=1,\dots,m. \tag{7}$$

Now multiplying both sides with $\mathbf{R}^{-\mathrm{T}}$ we obtain

$$\boldsymbol{\Sigma}_{\mathbf{X}}\mathbf{R}\tilde{\boldsymbol{\phi}}_i=\tilde{\lambda}_i\boldsymbol{\Sigma}_{\mathbf{V}}\mathbf{R}\tilde{\boldsymbol{\phi}}_i, \quad i=1,\dots,m, \tag{8}$$

which is the same generalized eigenvalue problem as described by Eq. (5) with $\boldsymbol{\phi}_i=\mathbf{R}\tilde{\boldsymbol{\phi}}_i$. Therefore, the new generalized eigenvectors or the SOMs for $\mathbf{Y}$ are

$$\tilde{\boldsymbol{\Phi}}=\mathbf{R}^{-1}\boldsymbol{\Phi}, \tag{9}$$

where the columns of *modal matrix* $\mathbf{\Phi}$ are composed of the original SOMs $\boldsymbol{\phi}_i$ and the columns of *modal matrix* $\tilde{\mathbf{\Phi}}$ are formed by the SOMs $\tilde{\boldsymbol{\phi}}_i$.

Another characteristic of the SOD is that the smoothness of SOCs is characterized by SOVs. This provides the SOD with a distinctive ability to differentiate SOCs according to their frequency content. The lower-frequency components result in smoother SOCs, while higher frequencies contribute to the jaggedness of the trends. To illustrate this point we will consider several examples and compare the performance of the SOD with the POD. In all the examples the columns of the matrix $\mathbf{X}$ will be composed of only one harmonic signal, since the SOD is invariant with respect to a nonsingular coordinate transformation.

For the first example we assemble the matrix $\mathbf{X}$ from time histories of several sinusoidal waveforms of the same amplitude but different frequencies. Let us say that columns of the matrix $\mathbf{X}$ are formed from the following signals: $x_k = \sin 20\pi kt$, where $k = 1, 2, \ldots, 10$. The resulting trajectory in the space of coordinates x_k is bounded with a sphere of radius one, since all coordinates oscillate with unit amplitude. Therefore, data variance in any spatial direction should be close to $1/2$, which should cause problems for the POD. We use a total of 334 points for each column sampled at $\Delta t = 3 \times 10^{-4}$. The results are shown in Fig. 1. It is observed that the SOD clearly identifies each signal by its frequency. In fact, from the obtained data depicted in Fig. 1(a) it is estimated that $\lambda_k \cong (20\pi k)^{-2}$ or the square root of the SOV approximates the reciprocal of the corresponding SOC's fundamental frequency $\omega_k = 20\pi k$. In contrast, as expected, the POD applied to the same matrix $\mathbf{X}$ cannot uniquely identify the principal directions of each component and yields confusing results.

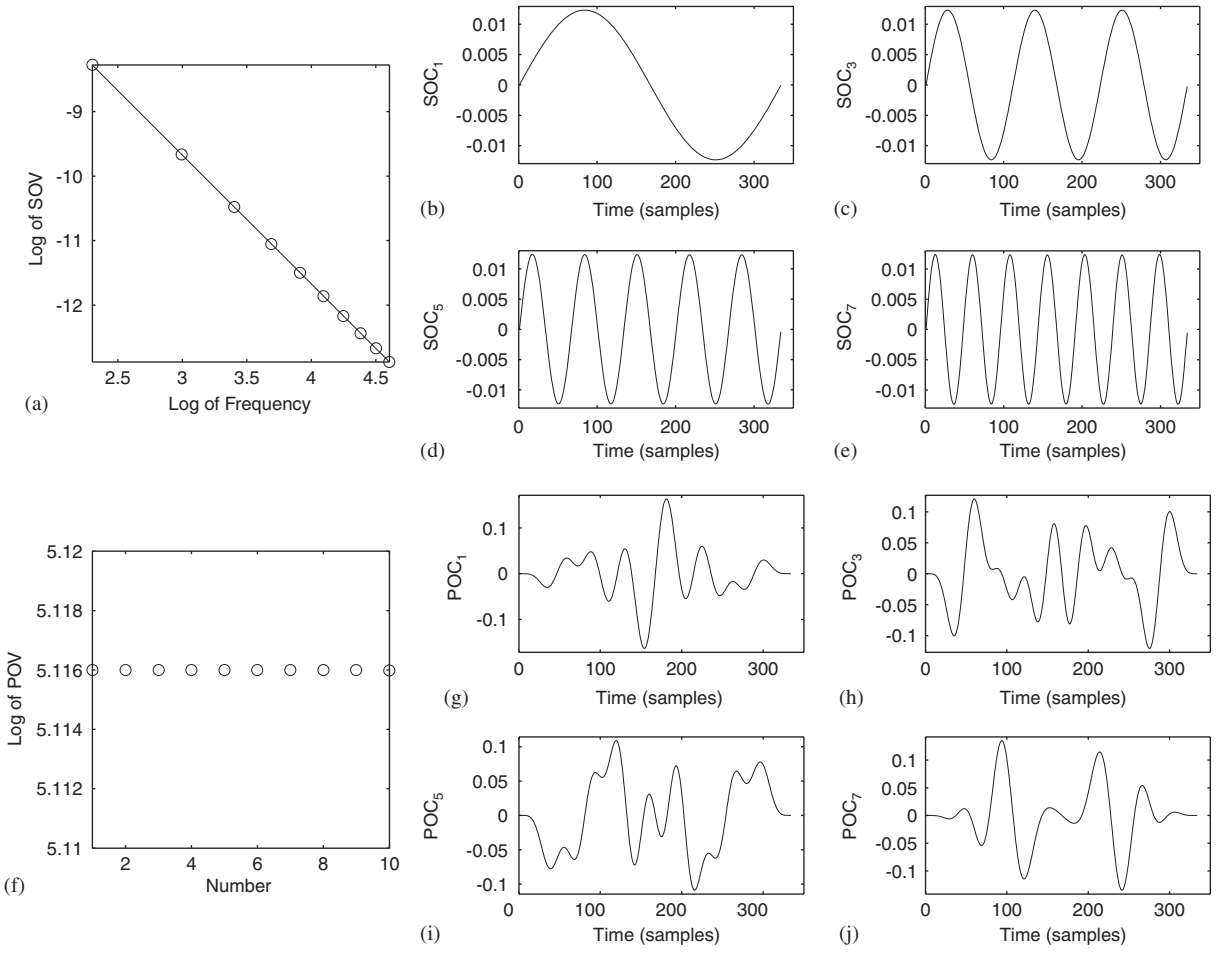

Fig. 1. Comparison of the SOD and POD performance in signal identification for $x_k = \sin 20\pi kt$, $k = 1, 2, \ldots, 10$. Plots (a)–(e) correspond to the SOD and plots (f)–(j) to the POD.

The observed relationship between the frequency and the SOV still holds for another example, where $\mathbf{X}$ is assembled from the same signals as in the example one, but with different amplitudes: $x_k = (11-k)\sin 20\pi kt$, $k = 1,\ldots,10$ (see Fig. 2). Now, our trajectory in the space of coordinates is bounded by the ellipsoid, major and minor axis of which are proportional to the signal amplitudes and are aligned along the corresponding coordinates. For this example we get exactly the same SOD results as for the first one, since each component still has the same distinct frequency. However, the POD now can also clearly identify all the signals from the matrix, since they have different amplitudes, and variances along the principal coordinates are distinct and identifiable. In this example singular values obtained through the POD analysis scale linearly with respect to the corresponding signal amplitudes.

In the final example, we look at the matrix $\mathbf{X}$ that is composed of $x_k = (11-k)\sin 2\pi 20t$, $k = 1,\ldots,10$, in which every column has exactly the same signal of different amplitudes (see Fig. 3). Therefore the matrix $\mathbf{X}$ is rank one and the corresponding trajectory in the space of coordinates is just an inclined straight line. Here, both the SOD and POD will fail to identify each of the components uniquely. However, the POD is still able to extract the characteristic shape of the signals as the first POC, since there is only one distinct maximum in variance along the direction of the inclined line in the space of coordinates. The SOD will fail to identify any trend in this case since both $\mathbf{\Sigma_X}$ and $\mathbf{\Sigma_V}$ are singular and rank one. Therefore, if the trajectory matrix $\mathbf{X}$ is rank one, the SOD-based identification will fail and one has to use the POD to identify the main trend in the data.

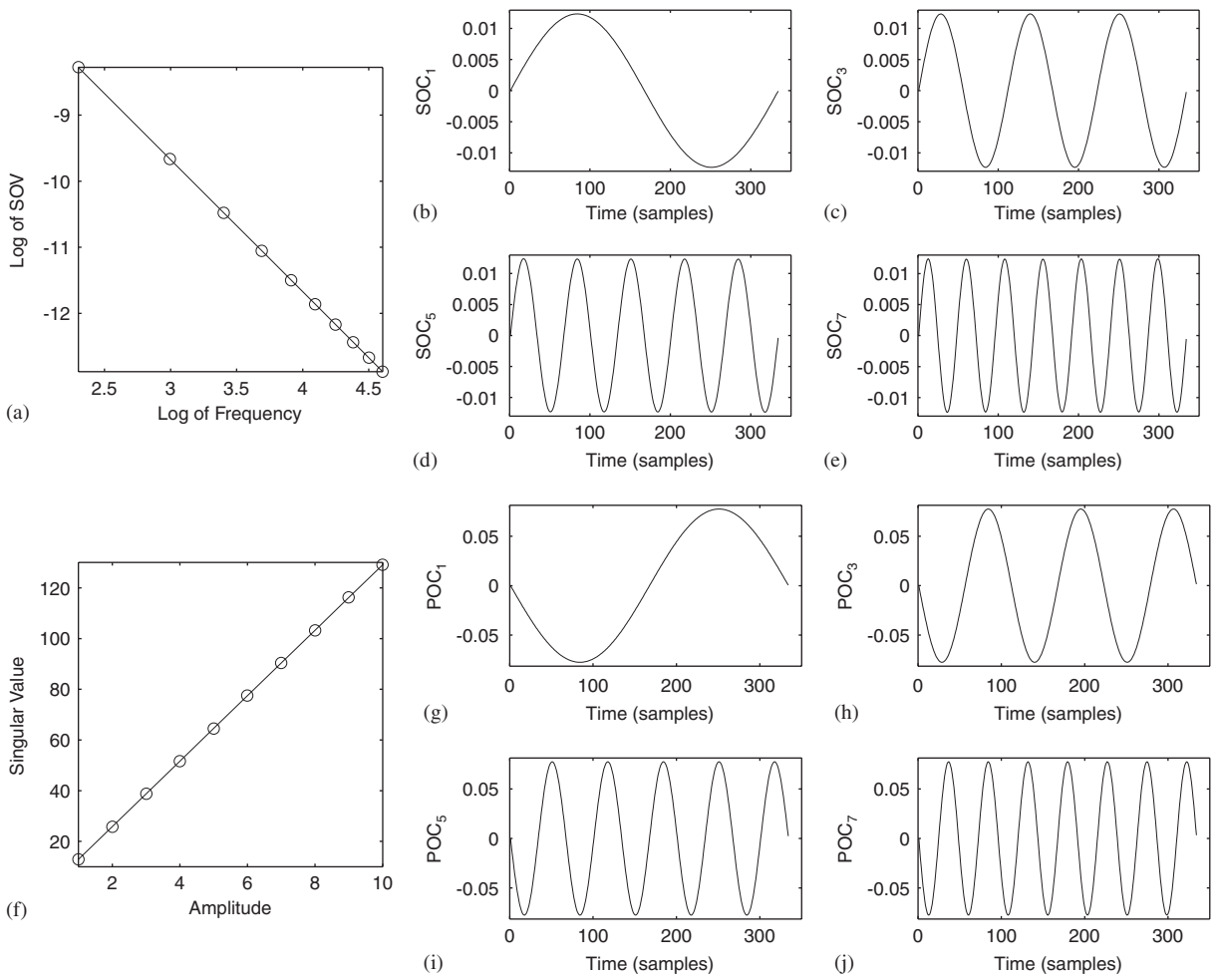

Fig. 2. Comparison of the SOD and POD performance in signal identification for $x_k = (11-k)\sin 20\pi kt$, $k = 1,\ldots,10$. Plots (a)–(e) correspond to the SOD and plots (f)–(j) to the POD.

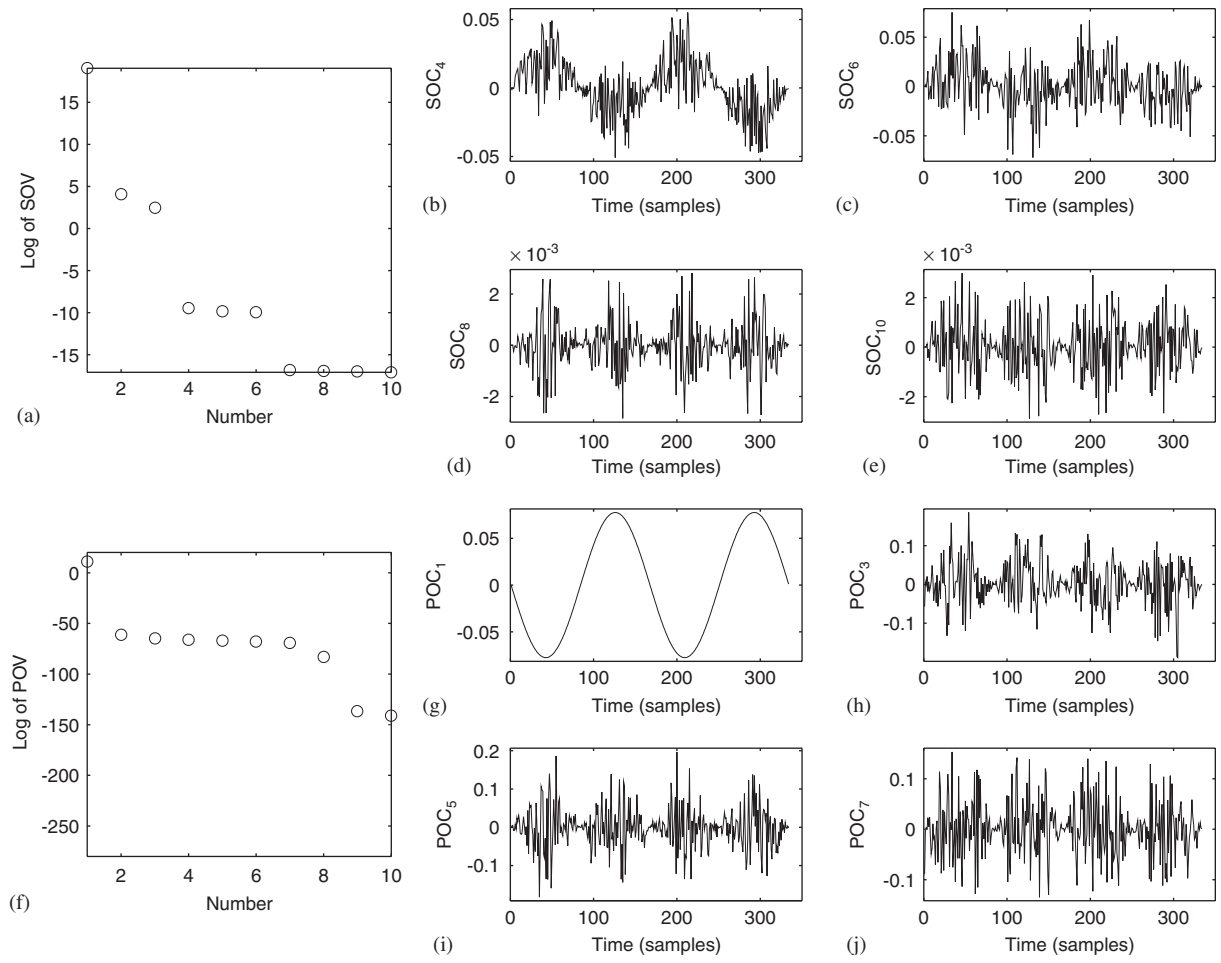

Fig. 3. Comparison of the SOD and POD performance in signal identification for $x_k = (11-k)\sin 2\pi 20t$, $k = 1,\ldots,10$. Plots (a)–(e) correspond to the SOD and plots (f)–(j) to the POD.

Usually one does not expect a rank one trajectory matrix, which can only arise through redundant measurements. Please note that even when the components of the trajectory matrix are of exactly the same form but differ in phase the SOD is still expected to work.

3. SOD-based modal analysis

By definition a normal mode shape describes the synchronous motion of the system when motions of all degrees of freedom are equi-periodic. The corresponding time histories or the modal coordinates give the time response of these synchronous motions. The response of a linear vibrational system is a superposition of these synchronous motions. Therefore, in modal analysis, we are looking at expanding the trajectory matrix $\mathbf{X}$ into the following two matrices:

$$\mathbf{X} = \mathbf{Q}\boldsymbol{\Psi}^{\mathrm{T}}, \tag{10}$$

where $\mathbf{Q} \in \mathbb{R}^{n\times m}$ is a matrix composed of modal coordinates and $\boldsymbol{\Psi} \in \mathbb{R}^{m\times m}$ is a modal matrix composed of corresponding LNMs. Therefore, the solution to the eigenvalue problem for a classical multi-degree-of-freedom undamped free vibration system,

$$\mathbf{M}\ddot{\mathbf{x}} + \mathbf{K}\mathbf{x} = \mathbf{0}, \tag{11}$$

satisfies the expression

$$\mathbf{K}\boldsymbol{\Psi} = \mathbf{M}\boldsymbol{\Psi}\boldsymbol{\Omega}, \tag{12}$$

where $\boldsymbol{\Omega}$ is a diagonal matrix of squares of the natural frequencies, ω_i^2, of the associated LNMs.

Now, considering the basic idea of the SOD expressed by Eq. (2),

$$\max_{\boldsymbol{\phi}} \left\{ \lambda(\boldsymbol{\phi}) = \frac{\|\mathbf{X}\boldsymbol{\phi}\|^2}{\|\mathbf{V}\boldsymbol{\phi}\|^2} = \frac{\boldsymbol{\phi}^{\mathrm{T}}\mathbf{X}^{\mathrm{T}}\mathbf{X}\boldsymbol{\phi}}{\boldsymbol{\phi}^{\mathrm{T}}\mathbf{X}^{\mathrm{T}}\mathbf{D}^{\mathrm{T}}\mathbf{D}\mathbf{X}\boldsymbol{\phi}} \right\} \tag{13}$$

and examining the term $\mathbf{D}^{\mathrm{T}}\mathbf{D}\mathbf{X}$ carefully, one can find that it is just an approximation of the negative acceleration matrix of $\mathbf{X}$

$$\mathbf{D}^{\mathrm{T}}\mathbf{D}\mathbf{X} \cong -\ddot{\mathbf{X}}. \tag{14}$$

The same acceleration matrix can be derived from Eq. (11) for a nonsingular mass matrix $\mathbf{M}$ as

$$\ddot{\mathbf{x}} = -\mathbf{M}^{-1}\mathbf{K}\mathbf{x} \quad \Rightarrow \quad \ddot{\mathbf{X}} = -\mathbf{X}\mathbf{K}^{\mathrm{T}}\mathbf{M}^{-\mathrm{T}}, \tag{15}$$

where $\mathbf{X}$ is the trajectory matrix of $\mathbf{x}$. Substituting this expression into Eq. (13), we have

$$\max_{\boldsymbol{\phi}} \frac{\boldsymbol{\phi}^{\mathrm{T}}\mathbf{X}^{\mathrm{T}}\mathbf{X}\boldsymbol{\phi}}{\boldsymbol{\phi}^{\mathrm{T}}\mathbf{X}^{\mathrm{T}}\mathbf{X}\mathbf{K}^{\mathrm{T}}\mathbf{M}^{-\mathrm{T}}\boldsymbol{\phi}}. \tag{16}$$

The solution to this maximization problem is obtained as before to yield

$$\mathbf{X}^{\mathrm{T}}\mathbf{X}\boldsymbol{\phi} = \lambda\mathbf{X}^{\mathrm{T}}\mathbf{X}\mathbf{K}^{\mathrm{T}}\mathbf{M}^{-\mathrm{T}}\boldsymbol{\phi}, \tag{17}$$

which further simplifies to

$$\mathbf{K}\boldsymbol{\Phi}^{-\mathrm{T}} = \mathbf{M}\boldsymbol{\Phi}^{-\mathrm{T}}\boldsymbol{\Lambda}. \tag{18}$$

Therefore, referring to Eq. (12), columns in $\boldsymbol{\Phi}^{-\mathrm{T}}$ give the LNMs and $\boldsymbol{\Lambda}$ is a diagonal matrix with its elements $\lambda_i = 1/\omega_i^2$ providing the natural frequency information.

4. Application of the SOD to discrete vibration systems

In order to compare the performance of the SOD with the POD in modal identification, we use the examples given in Ref. [7]. All the values used are exactly the same as in Ref. [7] unless it is noted explicitly.

4.1. Linear undamped free vibration

We consider a three-degree-of-freedom mass–spring system connected like it is shown in Fig. 4. The differential equation of motion for this system is the same as Eq. (11), with

$$\mathbf{M} = \begin{bmatrix} 2 & 0 & 0 \\ 0 & 1 & 0 \\ 0 & 0 & 1 \end{bmatrix} \quad \text{and} \quad \mathbf{K} = \begin{bmatrix} 2 & -1 & 0 \\ -1 & 2 & -1 \\ 0 & -1 & 1 \end{bmatrix}. \tag{19}$$

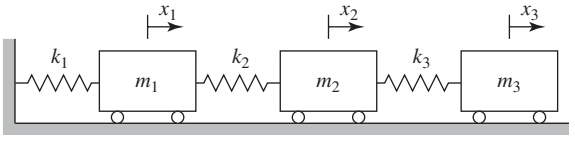

Fig. 4. A three-degree-of-freedom mass–spring vibration system.

The initial displacements are $\mathbf{x}(0) = [1, 0, 0]^{\mathrm{T}}$ and the initial velocities are $\mathbf{v}(0) = [0, 0, 0]^{\mathrm{T}}$. The LNMs assembled into a modal matrix are

$$\mathbf{\Psi} = \begin{bmatrix} 0.3602 & -0.7071 & 0.2338 \\ 0.5928 & 0.0000 & -0.8524 \\ 0.7204 & 0.7071 & 0.4676 \end{bmatrix}, \tag{20}$$

where each modal vector is unitary orthogonal with respect to the mass matrix. The corresponding modal frequencies are the square roots of the eigenvalues of the mass normalized stiffness matrix, that is $\omega_1 = 0.4209$, $\omega_2 = 1.0000$, and $\omega_3 = 1.6801$. Following the modal analysis steps, the modal initial conditions of the system are

$$\hat{\mathbf{x}}(0) = \mathbf{\Psi}^{-1}\mathbf{x}(0) = [-0.6777, 1.1547, 0.4554]^{\mathrm{T}}, \quad \hat{\mathbf{v}}(0) = \mathbf{\Psi}^{-1}\mathbf{v}(0) = [0, 0, 0]^{\mathrm{T}}, \tag{21}$$

where $\mathbf{\Psi}$ is now mass normalized. Then, the solution in modal coordinates is

$$\hat{\mathbf{x}}(t) = [-0.6777\cos(0.4209t),\ 1.1547\cos(t),\ 0.4554\cos(1.6801t)]^{\mathrm{T}} \tag{22}$$

and the solution in the original coordinates is $\mathbf{x}(t) = \mathbf{\Psi}\hat{\mathbf{x}}(t)$. The numerically obtained time series of the system vibration is used to form the trajectory matrix $\mathbf{X}$. Then $\mathbf{X}$ is used to form the covariance matrix $\mathbf{\Sigma}_{\mathbf{X}} = (1/n)\mathbf{X}^{\mathrm{T}}\mathbf{X}$.

For the POD-based modal analysis, $\mathbf{\Sigma}_{\mathbf{X}}$ needs to be pre-multiplied by the corresponding mass matrix $\mathbf{M}$ to obtain $\mathbf{\Sigma}_{\mathbf{X}}\mathbf{M}$ and the eigenvectors of $\mathbf{\Sigma}_{\mathbf{X}}\mathbf{M}$ are expected to converge to the LNMs of the vibration system [7]. For the SOD-based method, however, we only need the matrix $\mathbf{X}$ and $\mathbf{V}$ calculated by $\mathbf{DX}$ without knowing the mass matrix. In addition, the SOD also provides good estimates of the natural frequencies associated with the identified LNMs.

The results of this calculation are shown in Table 1. Here, the first column lists different sampling time steps used in the simulation and the second column shows the total number of samples used for each column of $\mathbf{X}$. The last three columns show the mean errors in estimating LNMs for both methods and the corresponding natural frequencies for the SOD. The errors for the estimated LNMs (E_{POD} and E_{SOD}) were calculated by taking the mean of the norm of the error in all identified modes, and the errors in the estimate of the natural frequencies (E_{ω}) are just the mean of all individual errors.

For this particular vibration system the SOD results are comparable to the POD results and in some cases substantially improve upon the latter. In addition, the SOD gives very accurate estimates of the natural frequencies associated with the identified LNMs. The errors in the estimates improve with the decrease in sampling time step and increase in the total number of points.

4.2. Linear free damped vibration

Here, we use the same vibration system as in the previous section but with the modal damping factors $\xi = 0.1$, 0.05 and 0.01 added to the system one by one. Here, the resultant system is simulated for each damping factor and both the POD- and SOD-based modal analyses are performed. The results are shown in Table 2. From these results it is apparent that for a damped system, as long as the frequencies associated with

Table 1
Mean of errors in identified modes and frequencies

Δt	Samples	E_{POD}	E_{SOD}	E_{ω}
0.2986	400	0.0042	0.0025	0.0070
0.1493	200	0.0511	0.0586	0.0027
0.1493	400	0.0065	0.0063	0.0011
0.1493	800	0.0044	0.0024	0.0012
0.1493	1600	0.0040	0.0022	0.0016
0.0746	1600	0.0044	0.0024	0.0008

the vibration modes are distinct and the sampled time history contains several periods, the SOD can successfully extract the active vibration modes and its performance is superior to the POD. This is especially true for the higher values of the damping factor.

For higher values of damping starting at about $\xi = 0.2$ the results for the SOD start to deteriorate ($E_{SOD} = 0.3846$ and $E_{POD} = 1.1562$). However, this is only true for the third highest mode. In fact, most of the increase in the error E_{SOD} in Table 2 can be attributed to this mode alone. The main reason for this deterioration is that this mode becomes highly damped and its effects are not apparent in the trajectory matrix. However, the quality of the first two SOMs remains at least as good as undamped POMs even for $\xi = 0.3$. Therefore, the SOD still can be used to correctly identify *active* vibration modes in a highly damped system.

4.3. Forced damped vibration system

For a forced damped vibration system, when the system is in a steady state, each of the masses vibrates with the same frequency. Therefore, all measured time series are equally smooth. This is very similar to the third case of the examples discussed in the SOD property section. However, each of the masses will oscillate with different phase, therefore avoiding the singularity observed in that example. When a system is not in resonance, there is no obvious energy distribution preference and neither POD nor SOD can extract the vibration modes. However, if the forcing frequency equals to one of the natural frequencies, the dominant vibration mode can be identified by either the POD or SOD. Table 3 lists some of the results for both methods. We again consider the system depicted in Fig. 4, except that a harmonic force of unit amplitude is applied to the first mass. The forcing frequency is taken to equal 1.6717, which matches the third damped modal frequency.

As described in Refs. [7,8], when one of the modes is in resonance we can use the directly obtained time series to form a matrix and perform the POD analysis without pre-multiplying the trajectory matrix by a corresponding mass matrix. The corresponding results from the POD are: the eigenvector for the damping factor equal to $\xi = 0.01$ is $[-0.2324, 0.8524, -0.4684]^T$ and the mean error norm is 0.0016. For modal damping $\xi = 0.05$, the eigenvector is given by $[-0.1934, 0.8513, -0.4878]^T$ and the mean error norm is 0.0451. When the damping factor goes to 0.1 the first eigenvector is $[-0.0200, 0.8360, -0.5483]^T$ and the mean error norm is 0.2291. We can see the performance of the raw-data POD is comparable to the POD procedure in the resonance conditions.

Table 2
Mean of errors for free damped vibration system

Δt	Samples	ξ	E_{POD}	E_{SOD}	E_ω
0.1493	400	0.1	0.2484	0.0611	0.0277
0.0746	800	0.1	0.1141	0.0622	0.0192
0.1493	400	0.05	0.0756	0.0197	0.0142
0.0746	800	0.05	0.0646	0.0168	0.0085
0.1493	400	0.01	0.0071	0.0071	0.0037
0.0746	800	0.01	0.0046	0.0039	0.0013

Table 3
Error means for forced damped vibration system

Δt	Samples	ξ	E_{POD}	E_{SOD}	E_ω
0.0746	800	0.10	0.2103	0.1694	0.0067
0.0746	800	0.05	0.0247	0.0110	8.5×10^{-4}
0.0746	800	0.01	8.4×10^{-4}	0.0074	0.0033

4.4. A case with comparable modal energies

Here, a particular case when the POD fails is investigated. As it was described in the introduction, when two POVs are comparable, the POD fails to uniquely identify the corresponding principal directions (case one in the examples for the SOD section). In this case, the SOD can be used as an alternative for extracting LNMs. Again, we use the example given in Ref. [7] to illustrate this point. All the parameters used are the same except

$$\mathbf{M} = \begin{bmatrix} 1 & 0 & 0 \\ 0 & 1 & 0 \\ 0 & 0 & 1 \end{bmatrix} \quad \text{and} \quad \mathbf{K} = \begin{bmatrix} 2 & -1 & 0 \\ -1 & 2 & -1 \\ 0 & -1 & 2 \end{bmatrix}. \tag{23}$$

The natural frequencies for this case are 0.7654, 1.4142, and 1.8478. The corresponding LNMs are

$$\mathbf{\Psi} = \begin{bmatrix} 0.5000 & -0.7071 & -0.5000 \\ 0.7071 & 0.0000 & 0.7071 \\ 0.5000 & 0.7071 & -0.5000 \end{bmatrix}.$$

The initial conditions are still $\mathbf{x}(0) = [1, 0, 0]^{\mathrm{T}}$ and $\mathbf{v}(0) = [0, 0, 0]^{\mathrm{T}}$. Again, after forming the trajectory matrix $\mathbf{X}$ (sampling time is 0.1493 and 400 sample points are used) we perform the POD and SOD analysis. The calculated POVs are 0.1236, 0.1264 and 0.2493 and the corresponding POMs are given by

$$\mathbf{\Psi}_P = \begin{bmatrix} 0.0763 & -0.6706 & -0.7379 \\ 0.9947 & 0.1018 & 0.0103 \\ 0.0682 & -0.7348 & 0.6748 \end{bmatrix}.$$

It can be seen that the POMs fail to correlate with the LNMs except maybe for the second mode. The corresponding SOMs are given by

$$\mathbf{\Psi}_S = \begin{bmatrix} 0.5043 & -0.7143 & 0.5158 \\ 0.7049 & 0.0007 & -0.7010 \\ 0.4988 & 0.6966 & 0.4924 \end{bmatrix}.$$

Here, we observe a much better approximation and the mean norm of the error for this SOD case is acceptably low: 0.0127. Therefore, the SOMs can still approximate the actual LNMs, while the POD fails to work in this case. In addition, the SOD also provides estimates of natural frequency: 0.7480, 1.4162 and 1.8355, which approximate the actual frequencies quite well.

5. Application to a distributed-parameter vibration system

A numerical simulation is also performed to validate the applicability of the proposed method in extracting modal parameters from a continuous vibration system. We consider a uniform cantilever beam clamped at $x = 0$ and free at $x = L$, where x is a spatial coordinate. All the parameters are the same as in [9]. That is, we assume a uniform mass per unit length $m(x) = 1$ with the stiffness of $EI = 1$ and the length of the beam $L = 1$. Ten sampling points are chosen along the beam equally spaced from $x = 0.1$ to $x = 1$. The corresponding initial lateral displacements at these points are assumed to be $[0.05, 0.05, 0.05, 0.05, 0.1, 0.12, 0.25, 0.5, 1, 2]$ and the initial velocities are set to zero. The characteristic equation for a cantilever beam is given by

$$\cos \beta L \cosh \beta L = -1, \tag{24}$$

where $\beta^4 = \omega^2$. The first ten successive values of β_r $(r = 1, \ldots, 10)$ are: 1.8751, 4.6941, 7.8548, 10.9955, 14.1372, 17.2788, 20.4204, 23.5619, 26.7035, and 29.8451. The corresponding eigenfunctions are in the following form

$$\psi_r(x) = A_r \left[\sin \beta_r x - \sinh \beta_r x - \frac{\sin \beta_r L + \sinh \beta_r L}{\cos \beta_r L + \cosh \beta_r L} (\cos \beta_r x - \cosh \beta_r x) \right], \quad r = 1, 2, \ldots . \tag{25}$$

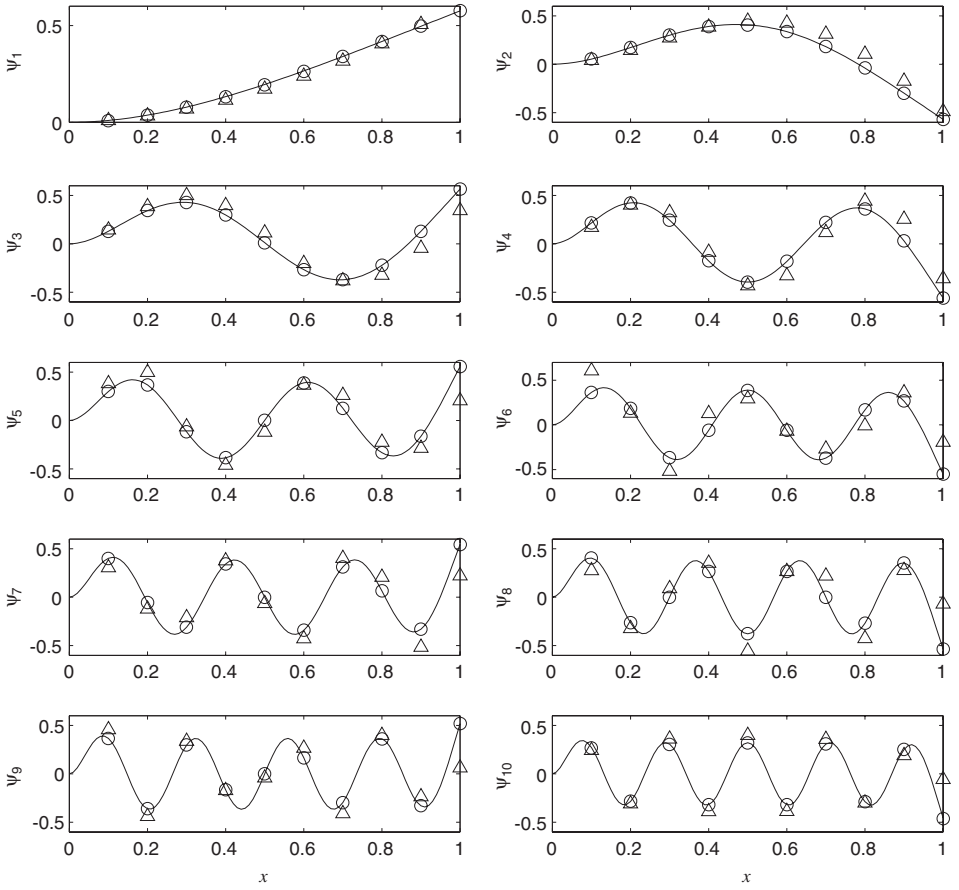

Fig. 5. Comparison of the POD- and SOD-based methods in extracting LNMs from a vibration scalar time series obtained using a model for a free vibration of a cantilever beam. The solid lines represent the actual LNMs, the △ correspond to the modes identified by the POD and the SOD results are given by ◯.

By using the ten initial displacements, we can determine the coefficients A_r $(r = 1, \ldots, 10)$ to be: $0.3480, -0.2213, 0.1389, -0.0598, 0.0463, -0.0166, 0.0227, -0.0141, 0.0112,$ and 0.0010. In order to use the POD- and SOD-based modal identification, we first need to form an ensemble matrix which is composed by the oscillation time series at the different sampling points along the beam. The sampling time $\Delta t = 0.00179$ and we use 3990 points to generate the displacement history. Following the established procedures for the POD- and SOD-based modal analysis, we can compare the 10 modes given by the POD and SOD to the actual LNMs. In the POD case, the norm of errors between these modes are: $0.0612, 0.2667, 0.3480, 0.3858, 0.4652, 0.5553, 0.4502, 0.6007, 0.5065, 0.4304$ respectively and the errors given by the SOD are: $0.0041, 0.0026, 0.0008, 0.0005, 0.0008, 0.0027, 0.0012, 0.0012, 0.0011, 0.0075$ respectively. The mean of all the errors for the POD case is 0.4070 and the same mean for the SOD is 0.0022, which shows two orders-of-magnitude improvement. Fig. 5 gives the visual comparison of the identified POD and SOD modes to the actual LNMs. In addition, the SOD-based method provides estimates for the corresponding natural frequencies: $3.5102, 21.9625, 61.6918, 120.6419, 198.7223, 294.8953, 407.2379, 532.4851, 665.5737, 799.2510,$ which give the following relative errors: $0.0017, 0.0033, 0.0001, 0.0022, 0.0057, 0.0124, 0.0239, 0.0426, 0.0714,$ and 0.1145 when compared to the actual natural frequencies.

6. Discussion

The results of the numerical study described in the previous section illustrate the application of the SOD to identifying LNMs of several simple vibration systems. In practical situations the choice of the correct

sampling time will be of critical value. Here, results for only two different sampling times of the vibration signals were provided. For the lumped-parameter vibration cases the largest sampling time used is well under the time interval dictated by the Nyquist's criteria. However, the results also show that the reduction of the sampling time considerably improves the quality of the identified natural frequencies and to a lesser extent the LNMs.

In general, the following general considerations need to be taken into account when choosing the sampling time. The Nyquist criteria associated with the highest modal frequency provides the upper limit on the sampling time, which will usually be quite large. The lower limit on the sampling time will be imposed by the total number of samples in each time series that can be analyzed, or m. For the SOD to work we need to capture at least one cycle of first mode oscillation. Therefore, the lower limit on the time step will be given by dividing the time period corresponding to this cycle by m. This might explain comparatively poor results for the lower modes in the distributed-parameter example, since only three complete first mode cycles are included in the data.

In the absence of noise the quality of the derivative matrix will always be better for smaller sampling times. However, in a noisy environment we expect to have some noise floor (approximately, corresponding to the time interval in which data is mainly dominated by noise) after which the reduction in time step will not bring any considerable improvement in quality. This can be mitigated by collecting several trajectory matrices and stacking them together in one trajectory matrix or doing ensemble average.

In many practical applications, most of the time, accelerations are measured instead of displacements. For linear systems the acceleration matrix can be obtained by appropriate nonsingular transformation of the displacement trajectory matrix; see Eq. (15). If the methodology described here is directly applied to the acceleration matrix, the results need to be interpreted using Eq. (9), where $\mathbf{R} = -\mathbf{K}^{\mathrm{T}}\mathbf{M}^{-\mathrm{T}}$. Therefore, for general applicability the acceleration matrix needs to be integrated to obtain the velocity and displacement matrices.

7. Conclusions

The ability of the POD to extract the principal components of a multivariate data set has made it a versatile tool frequently applied in engineering fields. Recent research interests have been focused on relating the POMs to the vibration modes and many authors have contributed to this area. Current research results show that the POMs converge to the linear vibration modes in the undamped free vibration case. This result is also applicable to the lightly damped vibration environment. Although these new findings shed light on a promising alternative to the traditional experimental modal analysis technique, there are several limitations to be addressed for the POD method to be used practically. The most important one is that the mass matrix of the system has to be known a priori, which is not always available in real application, especially for a distributed-parameter system. The other limitation is inherent in the POD analysis, that is, it cannot uniquely distinguish between the principal components that have comparable proper orthogonal values.

In this paper, a new multivariate data analysis tool (SOD) that overcomes the aforementioned limitations of the POD was presented. The SOD can be considered an extension of the POD, which acquires the ability to separate a multivariate data based on their characteristic frequency components. Mathematical justification for the SOD-based modal identification was given. Several detailed numerical examples were given to illustrate the SOD-based procedure, performance, and advantages. Specifically, it was shown that the SOD was invariant with respect to invertible coordinate transformation, which makes the SOD-based modal identification independent of a priori knowledge of the mass matrix. This also allows for convenient placement of transducers on structures of intricate shape.

Numerical simulations were used to show that for the undamped free vibration cases, lightly damped vibration and the distributed-parameter vibration case, the SOD yields the results that are comparable to or even better than those for the POD. In addition, the SOD does not require the determination of the mass matrix and can overcome the intrinsic limitation of the POD when the principal axes are not uniquely defined. In damped vibration cases it was observed that the SOD provided more accurate modal identification for higher damping ratios. In addition, the SOD provides accurate estimates of the natural frequencies for the identified modes.

Acknowledgements

This paper is based upon work supported by the National Science Foundation under Grant No. 0237792.

References

[1] D.S. Broomhead, G.P. King, Extracting qualitative dynamics from experimental data, *Physica D* 20 (1986) 217–236.
[2] A.M. Albano, J. Muench, C. Schwartz, Singular-value decomposition and the grassberger-procaccia algorithm, *Physical Review A* 38 (6) (1988) 3017–3026.
[3] S. Doclo, M. Moonen, SVD-based optimal filtering with applications to noise reduction in speech signals, in: *Proceedings of the 1999 IEEE Workshop on Applications of Signal Processing to Audio and Acoustics*, IEEE, New York, pp. 143–146.
[4] K. Shin, J.K. Hammond, P.R. White, Iterative SVD method for noise reduction of low-dimensional chaotic time series, *Mechanical Systems and Signal Processing* 13 (1) (1999) 115–124.
[5] P.K. Sadasivan, D.N. Dutt, SVD based technique for noise reduction in electroencephalographic signals, *Signal Processing* 55 (2) (1996) 179–189.
[6] P. Holmes, J.L. Lumley, G. Berkooz, *Turbulence, Coherent Structures, Dynamical Systems, and Symmetry*, Cambridge University Press, Cambridge, New York, 1996.
[7] B.F. Feeny, R. Kappagantu, On the physical interpretation of proper orthogonal modes in vibrations, *Journal of Sound and Vibration* 211 (4) (1998) 607–616.
[8] G. Kerschen, J.C. Golinval, Physical interpretation of the proper orthogonal modes using the singular value decomposition, *Journal of Sound and Vibration* 249 (5) (2002) 849–865.
[9] B.F. Feeny, On the proper orthogonal modes and normal modes of continuous vibration systems, *Journal of Vibration and Acoustics* 124 (1) (2002) 157–160.
[10] B.F. Feeny, Y. Liang, Interpreting proper orthogonal modes in randomly excited vibration systems, *Journal of Sound and Vibration* 265 (5) (2003) 953–966.
[11] S. Han, B.F. Feeny, Application of proper orthogonal decomposition to structural vibration analysis, *Mechanical Systems and Signal Processing* 17 (5) (2003) 989–1001.
[12] A. Chatterjee, J.P. Cusumano, D. Chelidze, Optimal tracking of parameter drift in a chaotic system: experiment and theory, *Journal of Sound and Vibration* 250 (5) (2002) 877–901.
[13] D. Chelidze, Identifying multidimensional damage in a hierarchical dynamical system, *Nonlinear Dynamics* 37 (2004) 307–322.
[14] D. Chelidze, M. Liu, Dynamical systems approach to fatigue damage identification, *Journal of Sound and Vibration* 281 (3–5) (2005) 887–904.